Journal of Novel Applied Sciences
Available online at www.jnasci.org
©2019 JNAS Journal-2019-8-3/63-70
ISSN 2322-5149 ©2019 JNAS

Influence of oxygen fugacity, temperature and pH on the Cu-ores, Bavanat area, SW Iran

Sina Asadi

Department of Earth Sciences, Faculty of Sciences, Shiraz University, Shiraz, Iran

***Corresponding author*:** Sina Asadi

ABSTRACT: In the Bavanat area, a large number of ore showings and deposits of epigenetic Cu-dominant mineralization exists. Quartz lodes and/or mineralized fault breccias are preferentially hosted in the Surian Permo-Triassic volcano-sedimentary complex. Their development is intimately related to faulting of presumable post early-Cimmerian orogeny (Middle to Late Triassic time; 240–220 Ma). Theoretical considerations concerning Cu solubility in hydrothermal-metamorphic system suggest that metal deposition might have involved low to moderate saline fluids previously responsible for metal scavenging in metabasite rocks at ca. 320-395ºC and $fO_2 < 10^{-40}$ (at pH = 4, $aCl^- \approx 3$ and $a(\Sigma S) = 0.001$). Copper deposition as chalcopyrite is expected to occur at ca. 230-310ºC under $10^{-34} < fO_2 < 10^{-29}$ as a result of different conditions.

***Keywords*:** Epigenetic Cu-lodes; Surian metamorphic complex; SW Iran.

INTRODUCTION

In the Bavanat area, there are a large number of ore-showings and deposits that show a relatively narrow variety of metal associations and have many features in common. They include epigenetic, structurally controlled sulfide ores, mostly in quartz veins along fault zones (usually N-S to NW-SE or ENE-WSW to E-W-trending strike-slip faults with normal component of movement), which are preferentially hosted in the Surian Permo-Triassic volcano-sedimentary complex (Asadi and Moore, 2017). According to data presented in many non-published technical reports, these ore-showings and deposits can be grouped in three major types characterized by the following metal associations Waring et al. (1998): I) Cu(-Ag, Au); II) Cu(-Ba-Zn, Pb, Ag); and III) Cu(-As, Ag, Au).

Many of these ore-showings were actively explored in the past and some deposits were extensively mined, particularly during the last decades (Asadi and Kolahdani, 2014a). Total metal production is difficult to calculate accurately, but the simple addition of the officially declared amounts (only available for some deposits) leads to minimum estimates of several thousands of tons of Cu-ore concentrates @0.9-3% Cu and several hundreds of tons of Zn-ore concentrates @1-4% Zn (the grades indicated for both metals represent the most common range of declared values); for Pb- and Au, Ag-ores the available information is very scanty and appears not to reflect suitably the actual production as qualitatively inferred on the basis of the mine tailings volume.

However, their widespread distribution and remarkable metal content (especially if the mineralogical nature of the ores, their distribution in lodes and the their average size is considered) pose important questions concerning the sources of metals and fluids, the reasons for a sustained high heat flow, the processes involved in metal transport and the mechanisms implicated in metal deposition. Answering these questions will improve significantly the current knowledge on the geodynamic and metallogenic evolution of the Surian Permo-Triassic volcano-sedimentary complex. The present work will focus only on a small part of the forth group of ore-showings and deposits that containing Cu-dominated mineralization.

This extended abstract reports the first results obtained in an ongoing research project that intends to examine the origin and evolution of the above mentioned epigenetic ore-forming systems. Work in progress and further research will enable to determine the compositional variability of the major mineral phases that form the mineralization and their host rocks, as well as to characterize in detail their bulk geochemical signature. These data, along with isotopic (stable and radiogenic; Asadi et al., 2013a, b; Asadi and Moore, 2017) determinations and results

of microthermometric and spectroscopic studies of fluid inclusions, will allow testing the hypotheses here articulated in a near future.

Geotectonic Setting

Crustal thinning during Neoproterozoic to Devonian times (e.g. Alric and Virlogeux 1977; Rachid Nejad-Omran et al., 2002; Alavi, 2004) has been suggested for the development of the volcanic and sedimentary layers in some areas of the SSZ (Alavi, 2004). In the studied area, the Permian carbonate, basic lava and synsedimentary breccia (Sheikholeslami et al., 2008) are interpreted to reflect an extensional tectonic regime, which is correlated with the separation of the central Iranian block from Gondwana (Berberian and King, 1981; Sheikholeslami et al., 2008).

During the early-Cimmerian orogeny (Middle to Late Triassic) the Tethyan oceanic lithosphere in the southern margin of Sanandaj-Sirjan zone, created along the accretion axis located to the SW, started to be consumed by oblique subduction under the central Iranian plate (Sheikholeslami et al., 2008). Following the subduction, two main regional metamorphic events and three main phases of deformation have been recognized in the Bavanat area (e.g., Hoseini, 2004; Orang and Mohajjel 2009). These Barrovian-type metamorphic events (Alric and Virlogeoux 1977; Houshmandzadeh and Soheili, 1990) are garnet-amphibolite to kyanite-quartz-mica schist and greenschist facies, respectively (Sheikholeslami et al., 2008). The deformation history probably included an early phase of nappe thrusting (D_1) which followed by open-style ductile folding and formation of a variably penetrative foliation cleavage (D_2). The third phase (D_3) occurred under conditions transitional between ductile and brittle deformation (Fattahi, 2012). D_3 deformation was associated with large-scale retrogressive hydration of amphibolites to greenschist facies assemblage (Fattahi, 2012). It is variably expressed by fracture cleavages, kink folds, crack-seal veins, and possibly large-scale transpressional faulting, and is largely overlapped with the main hydrothermal events that led to the silica alteration and copper ore emplacement.

The prograde metamorphic event during the early-Cimmerian discordance recorded the onset of the compression related to the peak of metamorphism (Sheikholeslami et al., 2008). Peak regional metamorphic mineral assemblages probably crystallized during D_2 deformation. According to Fazlnia et al. (2007) and using the U-Pb method, the thermo-barometric peak is inferred to have occurred at 187 ± 2.6 Ma. The peak pressure and temperature were estimated at 9.5 ± 1.2 kbar and 705 ± 40°C, respectively (Fazlnia et al., 2007). According to Paul et al. (2003) and Asadi et al. (2014b), the maximum crustal thickness reaches 65 km beneath the Sanadaj-Sirjan Zone at this time.

Uplift and cooling of the metamorphic complex during post-early Cimmerian orogeny (Middle Jurassic time; 159-167 Ma) has resulted in development of sedimentary and magmatic arc basins and the progressive acquisition of the ^{40}K–^{40}Ar age in the area (Sheikholeslami et al., 2008). The exhumation continued during the Jurassic and late Cimmerian orogeny with two consequences: the first, as highlighted above, was the progressive cooling of metamorphic minerals and infiltration of large volumes of hydrous fluids, which resulted in retrograde metamorphism (Sheikholeslami et al., 2008). The second consequence was the coeval development of retrograde metalliferous quartz veins in the Surian metamorphic complex.

Ore deposit geology

In the Bavanat area, the major deposits are Jian, Chir, Dideh Banki, and Mazayjan, all belonging to the Sanandaj-Sirjan metamorphic belt (Fig. 1). In the Jian deposit, the main lode (N35ºE, 75ºNW) shows a maximum thickness of 1.5m and was mined in an extent of 750 m up to ca. 150 m deep; two other lodes were identified (N-S, 45ºE and N-S, sub-vertical), although poorer in sulfides. All these lodes are preferentially hosted in metabasite rocks and are structurally controlled by a major NNE-SSW fault zone; secondary, sub-vertical E-W fault zones can also be observed (Asadi et al., 2013b). The most abundant sulfide minerals include chalcopyrite, pyrite, galena, sphalerite, with minor pyrrhotite (Fig. 2).

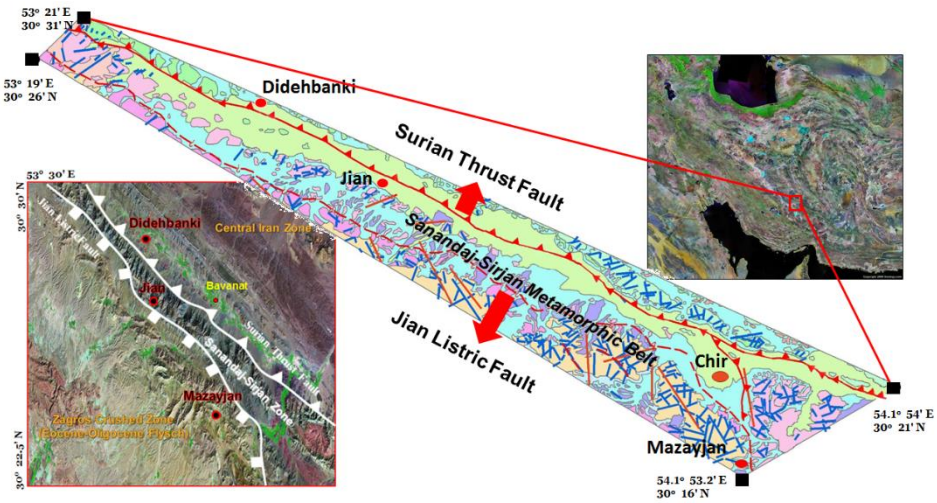

Figure 1. Simplified geological map of the Bavanat area, showing distribution of the Bavanat deposit and copper occurrences hosted in the Surian complex (Asadi and Moore, 2017)

In the Chir deposit, the main lode system has an average NNW-SSE trend, dips 50º-70ºE and was recognized in an extent of 3000m. A second lode of minor importance was also identified 430m eastwards of the major mineralized system, following an N-S trend and being enclosed in mafic metavolcanics (Asadi et al., 2013a).

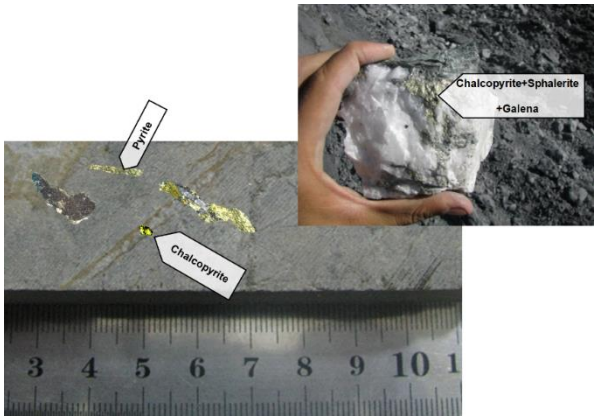

Figure 2. Drill core of an ore–bearing lode with disseminated pyrite+chalcopyrite+Sphalerite+galena

In the Dideh Banki deposit, the mineralized domain of the fault zone (N20ºW, 70ºE) is hosted in detrital metasediments of Surian complex. The lode can be followed for more than 1500m.
In the Mazayjan deposit, the main lode (<3m thick) follows a sub-vertical, N65ºE, left lateral fault zone, and is hosted in schists and greywackes of the Surian complex. Detailed geochemical mapping show that the lode comprises distinct zones of variable enrichment in different sulfides and/or sulfosalts, higher when greywackes are the host rocks.

Mineral Assemblages

All the Cu-lodes are mainly composed of different generations of both milky quartz and carbonates. The latter minerals make up distinct aggregates that form the vein-matrix along with quartz, and fill up diverse fracture systems whose relative chronology is difficult to establish. The main carbonate associations are: ankerite+dolomite+siderite in the Jian; calcite+ siderite in the Chir; dolomite+calcite in the Mazayjan; and ankrite+ siderite± dolomite in the Dideh Banki. Minor amounts of chlorite are also present in the Cu-lodes at Jian (filling up and intergranular microfractures only intersected by very late carbonate veinlets. Mineralized fault breccias, enclosing heterometric, angular and hydrothermally altered fragments of diverse host rocks, can be found in the Jian, Chir, Dideh Banki, and Mazayjan.

An accurate characterisation of primary ore mineralogy is presently a very difficult task because of the problematical access to the old mine works. However, a comprehensive inspection of samples collected in mine

tailings has led to results that are consistent with data presented in many technical reports contemporary of mining activity. In general, Jian ore mineralogy consists of copper-iron sulfides, sulfo-arsenides and sulfosalts, often with accessory amounts of lead and zinc sulfides. In the Dideh Banki, chalcopyrite and pyrite, with minor tennantite, tetrahedrite, sphalerite, pyrrhotite, galena is the main ore assemblage; chalcopyrite occurs as fractured masses developed mostly after pyrite but before chalcopyrite and tennantite- tetrahedrite, the latter often forming tiny grains deposited in late microfractures. At Chir and Mazayjan the mineral assemblage is apparently simple and contains just pyrite+tetrahedrite that develop coarse-grained aggregates randomly distributed in quartz-carbonate veins.

Generations cementing the angular rock-fragments in fault breccias; early quartz masses include fine disseminations of chalcopyrite, postdating the fractured grains of pyrite and tetrahedrit, locally associated with tennantite and rare sphalerite, occur in restricted matrix domains of the fault breccias, particularly in those subjected to intense late fracturing. The primary mineralization in Jian, the best-studied of this group of deposits (Asadi et al., 2013a), includes chalcopyrite, sphalerite, pyrrhotite, and galena; different generations of chalcopyrite can be identified, the early ones forming fractured masses (that may contain sphalerite, pyrrhotite relics) and the later ones consisting of coarse-grained aggregates that involve galena, which replace pyrite and are intimately related to siderite and dolomite deposition; a late pyrite generation develops together with galena and chalcopyrite, and these minerals can be observed in lately fractured domains of the lodes; as in other cases, tetrahedrite is uncommon but can be identified in some intensely fractured domains of the lodes, although always in those where galena is absent.

In all these deposits, an upper horizon of strong oxidation and hydration exists, often leading to a supergene metal enrichment zone of variable thickness that comprises mixtures in diverse proportions of secondary oxides, hydroxides, sulfates, phosphates, arsenates, native copper, hydrated Cu-bearing silicates and carbonates, and occasionally also secondary sulfides. Argillic minerals also occur as silicified argillic haloes in the outer zones of ore-bearing quartz veins. Some veins are characterized by the occurrence of large rutile needles (0.2–1 mm in diameter and up to 30 mm in length) and lack of sulfide minerals.

As referred to above, the access to the old mine works is currently very difficult, thus limiting any sampling programmable enough to characterize properly both the primary ore mineralogy and its bulk chemical composition. The geochemical data existing at present are, therefore, insufficient and further sampling efforts should be made in order to analyze drill-core samples when available. Nevertheless, a brief review of data available shows that: 1) in the Jian, strongly oxidized and leached horizon have 1852-30157 ppm Cu, 716-8154 ppm As, and <200 ppb to 3.4 ppm Au; the host schist with fracture infillings composed of secondary Cu-minerals hold 6.5% Cu, 3415 ppm As, and 3.3 ppm Au; 2) in the Dideh Banki, oxide ore minerals may reach 4% Cu, 1630 ppm As, and 783 ppb Au, whereas mineralized fault breccias display 2.5% Cu; 3) in the Chir, the Cu-content of fault breccias with secondary Cu-minerals reaches 7343 ppm, going up to 2.1% in strongly weathered samples; 4) in the Mazayjan, fault breccias with fine chalcopyrite and pyrite disseminations show 6.3% As, 1.7 ppm Au, and 4750 ppm Zn, and according to old technical reports primary ores contain, on average, 1.1% Cu.

Discussion

1. Ore mineralization

Field evidence indicates that the Cu-dominant mineralization here concisely described is intimately associated with faulting. This faulting dates presumably from Late-Triassic times, but precise dating of fault rocks and ore minerals is needed to establish this with certainty, which means that a late hydrothermal contribution during Early-Cimmerian orogeny cannot be precluded. Field relationships and the mineralogical-textural characteristics shown by quartz lodes, mineralized breccias and host-rocks, also point to an epigenetic origin of this mineralization. The zoned structural and/or mineralogical character (sometimes following a rhythmic pattern) displayed by many lodes, as well as the polyphase fragmentation revealed by many fault breccias, are taken as evidence for a repeated seismic activity of the major faults and a multi-stage circulation of mineralizing, hydrothermal fluids. From this, one may conclude that, as expected, fluid flow focusing within faults is particularly important in areas of highest fracture density and opening, such as damage zones associated with fault jogs, bends and splays. Therefore, fluid-driven growth of hydraulically linked networks of faults and fractures is favored through constructive interplays between deformation, fluid flow, and fluid pressure.

Macroscopic fluid pathways in fractured-controlled hydrothermal systems are influenced by the evolving connectivity among structural elements during progressive deformation, the most extreme flow focusing occurring at the onset of a system-wide fluid flow for which a percolation threshold is attained. This threshold value requires bulk strains as low as a few percent, but in the presence of rocks with contrasting mechanical behavior, such as alternating sequences of greywackes and schists, the more competent rock domains will yield much earlier for a fixed temperature and strain rate, becoming gradually the preferential host of mineralization, as observed at Jian, Dideh Banki, and Mazayjan. In relatively schist series, the prior development of a fracture network is needed to achieve the

critical percolation threshold for lodes formation, preventing the dispersion of the mineralizing fluid flow. This contrasting behavior helps to explain the widespread distribution of a relatively high number of ore showings among which only a few important lodes can indeed develop.

From observation, data results and numerical modeling, it is known that fluid pressure gradients, buoyancy effects and permeability distribution are the main parameters that control the fluid pathways between metal sources and the sites of hydrothermal-ore deposition. Active deformation is therefore needed to generate and maintain permeability, and to sustain large-scale fluid flow, provided that anomalous heat flow exists. In these conditions, broad gradients produced by buoyancy or fluid pressure will enhance long distance fluid flow provided that the local perturbations have less magnitude than the broad anomalies thus generated. This would control both the extent and the lifetime of large-scale hydrothermal systems, favoring also the processes of metal scavenging from substantial rock volumes. Local, small fluid flows around structural discontinuities, such as faults and/or fracture arrays of variable complexity, will favor, conversely, the tendency for flow focusing, controlling the deposition of metals. In conclusion, hydrothermal fluids are, expectably, mixtures in variable proportions of chemically modified meteoric waters and residual metamorphic solutions, having extracted their metal contents mainly from Palaeozoic metasediments and mrtabasites. Accepting this work-hypothesis, it is important to discuss what are the most suitable physical and chemical conditions for copper leaching and transport? Thus constraining some of the most important parameters that may rule the development of Cu-dominant mineralization.

2. Active copper transport: temperature, pH and fO_2 values

The estimated fO_2 values of 10^{-34} to 10^{-29} bars are listed in Table 1. The most likely conditions of Cu transport in hydrothermal conditions can be roughly evaluated in function of temperature and fO_2 values, by changing iteratively the pH, aCl^- and a(ΣS) of hydrothermal solutions and considering the most stable ionic Cu-complexes (namely $CuCl^0$, $CuCl^{3-}$ and $Cu(HS)^{2-}$). Since the Palaeozoic metavolcano-sedimentary sequences in the Bavanat area include abundant mafic schists, a reduced ($SO_4/H_2S<1$) environment for Cu leaching and transport is largely favored. Additionally, the widespread evidence of feldspar hydrolysis points out to an acidic environment, thus suggesting that Cl-complexes would control copper solubility, being the relative predominance of $CuCl^{3-}$ over $CuCl^0$ a direct consequence of fluid salinity increase. From this it may be concluded that leaching and transport of Cu will be very significant at ca. 320-395ºC for $fO_2<10^{-40}$, if pH = 4, $aCl^- \approx 3$ and a(ΣS) = 0.001.

Table 1. Calculated bulk composition and oxygen fugacity for liquid-carbonic inclusions in ore-bearing quartz lode from Bavanat area

Location	Phase	XCO_2	XH_2O	XNaCl	Log fO_2
Jian	L_1+L_2+V	0.175	0.794	0.0309	-29.9
Jian	L_1+L_2+V	0.12	0.871	0.008	-29.5
Jian	L_1+L_2+V	0.146	0.839	0.014	-31.2
Jian	L_1+L_2+V	0.12	0.859	0.02	-29.8
Jian	L_1+L_2+V	0.206	0.779	0.014	-29.9
Jian	L_1+L_2+V	0.146	0.844	0.009	-29.7
Jian	L_1+L_2+V	0.175	0.813	0.011	-34.0
Jian	L_1+L_2+V	0.073	0.895	0.031	-29.1
Jian	L_1+L_2+V	0.146	0.831	0.022	-29.4
Jian	L_1+L_2+V	0.75	0.81	0.014	-29.2
Jian	L_1+L_2+V	0.12	0.865	0.014	-29.1
Jian	L_1+L_2+V	0.207	0.784	0.008	-29.3
Jian	L_1+L_2+V	0.12	0.848	0.031	-32.9
Jian	L_1+L_2+V	0.175	0.798	0.026	-31.4
Jian	L_1+L_2+V	0.146	0.827	0.026	-29.8
Jian	L_1+L_2+V	0.12	0.862	0.017	-29.0
Mazayjan	L_1+L_2+V	0.073	0.914	0.012	-29.5
Mazayjan	L_1+L_2+V	0.12	0.871	0.008	-33.1
Mazayjan	L_1+L_2+V	0.034	0.955	0.011	-31.1
Mazayjan	L_1+L_2+V	0.073	0.908	0.017	-29.4
Mazayjan	L_1+L_2+V	0.241	0.731	0.027	-29.9
Mazayjan	L_1+L_2+V	0.175	0.798	0.026	-29.0
Mazayjan	L_1+L_2+V	0.175	0.796	0.029	-32.9
Mazayjan	L_1+L_2+V	0.206	0.766	0.027	-30.7
Mazayjan	L_1+L_2+V	0.12	0.85	0.029	-31.3
Dideh Banki	L_1+L_2+V	0.073	0.906	0.02	-33.7
Dideh Banki	L_1+L_2+V	0.175	0.806	0.018	-33.2
Dideh Banki	L_1+L_2+V	0.12	0.868	0.011	-32.4
Dideh Banki	L_1+L_2+V	0.073	0.914	0.011	-30.3
Dideh Banki	L_1+L_2+V	0.175	0.804	0.02	-29.1

Dideh Banki	L_1+L_2+V	0.12	0.855	0.025	-30.4
Dideh Banki	L_1+L_2+V	0.073	0.919	0.006	-32.4
Dideh Banki	L_1+L_2+V	0.073	0.904	0.022	-33.3
Dideh Banki	L_1+L_2+V	0.074	0.904	0.021	-30.2
Chir	L_1+L_2+V	0.034	0.932	0.033	-29.8
Chir	L_1+L_2+V	0.073	0.915	0.011	-29.7
Chir	L_1+L_2+V	0.073	0.905	0.021	-32.5
Chir	L_1+L_2+V	0.034	0.94	0.026	-33.2
Chir	L_1+L_2+V	0.073	0.9	0.026	-29.6
Chir	L_1+L_2+V	0.073	0.903	0.022	-29.5
Chir	L_1+L_2+V	0.12	0.857	0.022	-30.8
Chir	L_1+L_2+V	0.0737	0.905	0.021	-32.0
Chir	L_1+L_2+V	0.12	0.864	0.015	-34.7

Notes: XCO_2, XH_2O, XNaCl= mole fractions of CO_2, H_2O and NaCl estimated from microthermometric data and Log fO_2= oxygen fugacity estimated from the reaction $CH_{4(g)} + 2O_{2(g)} \Leftrightarrow CO_{2(g)} + 2H_2O_{(g)}$ for H_2O-CO_2-bearing inclusions.

Ore–forming fluids are generally above the CO_2/CH_4 and below the SO_4/H_2S buffer boundaries throughout ore mineralization. The pH range of the hydrothermal fluids can be set by the stability of pyrite at temperatures of 243 to 386°C. Within this range, copper solubility decreases rapidly with a little increase in pH (Yoo et al., 2011; Tale Fazel et al. 2015). Such an increase could occur during fluid immiscibility due to the partitioning of acidic components (e.g., HCl, CO_2, and SO_2) into the vapour phases (Heinrich et al., 1989; Dugdale and Hagemann 2001; Urban et al., 2006; Yoo et al., 2011; Bodnar et al., 2014). The obtained values are consistent with the observed ore mineral assemblages (i.e. chalcopyrite+ pyrite± sphalerite± galena) from the Bavanat Cu-lodes.

Among the fluid inclusions (Table 1), the range of XCO_2/XCH_4 ratios may be interpreted as fluids evolving from less reduced, high XCO_2/XCH_4, relatively high fO_2 to more reduced, lower XCO_2/XCH_4, relatively low fO_2 compositions as they react with metamorphic rocks around the fractures (Cox et al., 1995). These results are consistent with the majority of reduced greenschist deposits (Fig. 3) in the world (e.g., Anderson et al., 2004; Phillips and Powell, 2010; Evans and Battles, 2011).

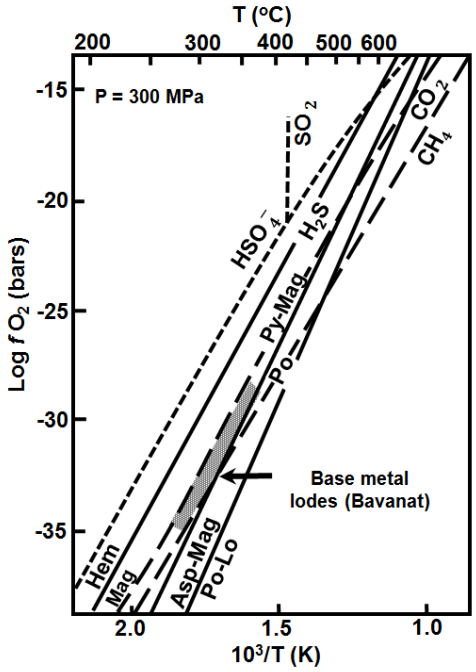

Figure 3. Log fO_2 vs. temperature diagram of ore–forming fluids at the P=300 MPa condition for the Bavanat area. Ore–forming fluid compositions are plotted below the hematite/magnetite and SO_2/H_2S buffers and above the CO_2/CH_4 buffer (after Urban et al., 2006). Py= pyrite, Asp = arsenopyrite, Hem = hematite, Lo = loellingite, Mag = magnetite, Po= pyrrhotite.

Under these chemical conditions, other metals (e.g., Zn, Pb, Ag, As, and Au) can also be efficiently carried in hydrothermal solutions, provided that they exist also in metabasits-metasediments.

Conclusions

The Bavanat Cu deposit is a shear zone–controlled lode system. In this system, the deposition of chalcopyrite usually postdates pyrite development, although post-chalcopyrite associated to minor amounts of sphalerite and galena is also known, when recorded, is typically an early process; the growth of tennantite and tetrahydrite, on the contrary, is very restricted and seems to take place lately. On the basis of these observations and the afore-mentioned hypothetical characteristics of hydrothermal solutions, one may conclude that chalcopyrite mineralization will be strongly favored at temperature conditions of ca. 310-385ºC under $10^{-34} < fO_2 < 10^{-29}$, for a wide range of fluid salinities (8≤wt.% NaCl equivalent≤18). Also, chalcopyrite deposition can be envisaged as a result of local temperature decrease and/or H_2S concentration increase and/or salinity depletion and/or reduction and/or pH rise. Many of these processes can easily be attained if local system depressurisation, fluid mixing and/or common fluid/rock interactions are considered, all of them geologically plausible and compatible with faulting during crustal uplift. For that narrow temperature range (ca. 270-312ºC), Zn and Pb will remain mostly in solution, thus explaining the scarcity of galena and sphalerite in the lodes, as well as their late deposition under lower temperature conditions. In this scenario, very small amounts of Au, As, and Ag are also expected to deposit.

Acknowledgments

I am indebted to many of my friends, colleagues and students who have helped me in various ways. The authors would like to thank Managing director of Bavanat Corporation Ltd. for his help during fieldwork and sampling.

REFERENCES

Alavi M (2004) Regional Stratigraphy of the Zagros Fold-Thrust Belt of Iran and Its Proforeland Evolution. American Journal of Science, 304, 1–20.

Alric G, Virlogeux D (1977) Pétrographie et géochimie des roches métamorphiques et magmatiques de la région de Deh Bid–Bavanat, Chaîne de Sanandaj–Sirjan, Iran, Thèse 3ème cycle, Grenoble, France, Université scientifique et médicale de Grenoble, 316 p.

Anderson R, Graham CM, Boyce AJ, Fallick AE (2004) Metamorphic and basin fluids in quartz–carbonate–sulphide veins in the SW Scottish Highlands: a stable isotope and fluid inclusion study. Geofluids, 4, 169–185.

Asadi S (2018) Triggers for the generation of post–collisional porphyry Cu systems in the Kerman magmatic copper belt, Iran: New constraints from elemental and isotopic (Sr–Nd–Hf–O) data. Gondwana Research, 64, 97-121.

Asadi S, Kolahdani S (2014a) Tectono-magmatic evolution of the Lut block, eastern Iran: A model for spatial localization of porphyry Cu mineralization. Journal of Novel Applied Sciences, 3, 1058-1069.

Asadi s, Mathur R, Moore F, Zarasvandi A (2015) Copper isotope fractionation in the Meiduk porphyry copper deposit, Northwest of Kerman Cenozoic magmatic arc, Iran. Terra Nova, 27, 36-41.

Asadi S, Moore F (2017) Fluid evolution in H_2O–CO_2–NaCl system and metallogenic analysis of the Surian metamorphic complex, Bavanat Cu deposit, Southwest Iran. Mineralogy and Petrology, 111, 145-161.

Asadi S, Moore F, Fattahi N (2013a) Fluid inclusion and stable isotope constraints on the genesis of the Jian copper deposit, Sanandaj–Sirjan metamorphic zone, Iran. Geofluids, 13, 66-81.

Asadi S, Moore F, Zarasvandi A (2014b) Discriminating productive and barren porphyry copper deposits in the southeastern part of the central Iranian volcano–plutonic belt, Kerman region, Iran: A review. Earth–Science Reviews, 138, 25–46.

Asadi S, Moore F, Zarasvandi A, Khosrojerdi M (2013b) First report on the occurrence of CO_2-bearing fluid inclusions in the Meiduk porphyry copper deposit, Iran: implications for mineralisation processes in a continental collision setting. Geologos, 19, 301-320.

Berberian M, King GCP (1981) Towards a paleogeography and tectonic evolution of Iran. Canadian Journal of Earth Sciences, 18, 210–285.

Bodnar RJ, Lecumberri–Sanchez P, Moncada D, Steele–MacInnis M (2014) Fluid inclusions in hydrothermal ore deposits. In: Holland HD, Turekian KK (eds) Treatise on geochemistry, 2nd edn. Elsevier Science and Technology, Oxford, pp 119–142.

Cox SF, Sun SS, Etheridge MA, Wall VJ, Potter TF (1995) Structural and geochemical controls on the development of turbidite–hosted gold quartz vein deposits, Wattle Gully mine, Central Victoria, Australia. Economic Geology, 90, 1722–1746.

Dugdale AL, Hagemann SG (2001) The Bronzewing lode–gold deposit, Western Australia: P–T–X evidence for fluid immiscibility caused by cyclic decompression in gold–bearing quartz veins. Chemical Geology, 173, 59–90.

Evans AM, Battles DA (2011) Fluid inclusion and stable isotope analyses of veins from the central Appalachian Valley and Ridge province: Implications for regional synorogenic hydrologic structure and fluid migration. Geological Society of America Bulletin, 12, 1841–1860.

Fattahi N (2012) Geochemistry and genesis of copper mineralization in Surian Complex, Jian area (Bavanat, Fars Province). Unpublished M.sc. thesis in Economic Geology, Shiraz University, 186p.

Fazlnia A, Moradian A, Rezaei K, Moazzen M, Alipour S (2007) Synchronous Activity of Anorthositic and S-type Granitic Magmas in Chah-Dozdan Batholith, Neyriz, Iran: Evidence of Zircon SHRIMP and Monazite CHIME Dating. Journal of Sciences, Islamic Republic of Iran, 18, 221-237.

Heinrich CA, Andrew AS, Wilkins RWT, Patterson DJ (1989) A fluid inclusion and stable isotope study of synmetamorphic copper ore formation at Mount Isa, Australia. Economic Geology, 84, 529-550.

Hoseini A (2004) Petrological and deformational studies on regional metamorphic rocks of the Koresefid area, north east of Neyriz. Unpublished M.Sc. thesis, Tabriz, Iran, Tabriz University, 1820 p.

Houshmandzadeh A, Soheili M (1990) Description of Eqlid map. Geological Survey of Iran, no.G10, 157 p.

Orang K, Mohajjel M (2009) Polyphase deformation at Chahgaz area, south of Shahre Babak. Conference of the Geological Society of Iran, 12th symposium, Ahvaz, 102–103.

Paul A, Kaviani A, Hatzfeld D, Mokhtari M (2003) Lithospheric structure of central Zagros from seismological Tomography. Four International Conferences of Earthquake engineering and Seismology, 12–14 may, Tehran, Iran.

Phillips GN, Powell R (2010) Formation of gold deposits: A metamorphic devolatilization model. Journal of Metamorphic Geology, 28, 689–718.

Rachid Nejad-Omran N, Hachem Emami M, Sabzehei M, Rastad E, Bellon H, Pique A (2002) Lithostratigraphie et histoire pale´ozoı¨que a` pale´oce`ne des complexes me´tamorphiques de la re´gion de Muteh, zone de Sanandaj-Sirjan (Iran me´ridonal), Geoscience, 334, 1185–1191.

Sheikholeslami MR, Pique A, Mobayen P, Sabzehei M, Bellon H, Emami MH (2008) Tectono-metamorphic evolution of the Neyriz metamorphic complex,Quri-Kor-e-Sefid area (Sanandaj-Sirjan Zone, SW Iran). Journal of Asian Earth Sciences, 31, 504–521.

Tale Fazel E, Mehrabi B, Tabbakh Shabani AA (2015) Kuh-e Dom Fe–Cu–Au prospect, Anarak Metallogenic Complex, Central Iran: a geological, mineralogical and fluid inclusion study. Mineralogy and Petrology, 109, 115-141.

Urban MTR, Hurai V, Konecny P, Chovan M (2006) Superdense CO_2 inclusions in Cretaceous quartz–stibnite veins hosted in low–grade Variscan basement of the Western Carpathians, Slovakia. Mineralium Deposita, 40, 867–873.

Waring CL, Heinrich CA, Wall VJ (1998) Proterozoic metamorphic copper deposits. Journal of Australian Geology and Geophysics, 17, 239-246.

Yoo BC, Brown PE, White NC (2011) Hydrothermal fluid characteristics and genesis of Cu quartz veins in the Hwanggangri metallogenic district, Republic of Korea: Mineralogy, fluid inclusion and stable isotope studies. Journal of Geochemical Exploration, 110, 245–259.